CrystEngComm

Accepted Manuscript

ROYAL SOCIETY OF CHEMISTRY

www.rsc.org/crystengcomm

Journal Name

ARTICLE

Received 00th January 20xx,
Accepted 00th January 20xx

DOI: 10.1039/x0xx00000x

www.rsc.org/

Polyanionic Clusters Embedded in Lattice-type Hydrogen Bonding Network Involving In Situ Bond Activation and Coupling of Organic Cation

Zhan-Gang Han*, Yun-Ping Liu, Xiao-Fang Zhao, Jin-Shuang Yan and Xue-Liang Zhai

Two inorganic-organic supramolecular polyoxometalates, $(H_2chtpy)_2[SiW_{12}O_{40}]$ (**1**) (chtpy= 1,3,4,6-tetra(4-pyridyl)cyclohexane-1,3-diol) and $[Co(Hbztpy)_2]H[AlW_{12}O_{40}]\cdot 3H_2O$ (**2**) (bztpy= 1,2,4,5-tetra(4-pyridyl)benzene) have been hydrothermally synthesized and characterized. Both of them consist of complex supramolecular contacts between inorganic polyanions and organic cations. During the formation process of **1** and **2**, in situ organic reactions involving C-C coupling through dehydrogenative cyclodimerization of two flexible 1,3-bis(4-pyridyl)propane (bpp) molecules were observed. The tetradentate pyridyl chtpy and bztpy serve as 4-connected nodes to enrich the structural topologies of **1-2**. The typical centered N-H…N (N…N = 2.6-2.7 Å) hydrogen bonding interactions link organic cations to form grid-type networks for capturing the pseudo-spherical Keggin-type anions. The pH values of reaction solutions are important for the intermolecular C-C coupling of organic molecules, and their transformation mechanisms are discussed.

1. Introduction

Recent studies have revealed that under pressure and at low temperatures, in situ organic reaction with the presence of transition metal centers is an effective method not only to generate organic molecules/ligands that are difficult to be synthesized through conventional methods, but also to represent a potential direction for the design and construction of new inorganic-organic frameworks in crystal engineering.[1] As an important bridge between coordination chemistry and organic chemistry, in situ metal/ligand reactions have been extensively developed to investigate the generation of novel coordination networks, the elucidation of reaction mechanisms, as well as the discovery of new organic reactions unable to be prepared under normal reaction.[2-4] Particular attention has also been recently devoted to the entangled systems because of their potential applications as materials for gas storage, separation, and catalysis.[5]

Polyoxometalates (POMs) with the unrivalled structural diversities and intriguing physicochemical properties have become one of the most rapidly developing areas in inorganic chemistry and materials science.[6-9] In materials chemistry, POMs as green molecular catalysts usually display excellent catalysis performance for many organic reactions. Therefore, it might be expected to test the probability introducing POMs into the in situ organic reaction under hydrothermal systems. Some POM-based compounds involving the in situ formation of organic ligands have been reported,[10] which have drawn great attention because of their undisputed beauty and novel configuration. It has been known that 1,3-bis(4-pyridyl)propane (bpp) with various structural features for its length and flexibility of $–(CH_2)_3–$ is a good candidate for the construction of inorganic-organic hybrids.[11] In 2012, our group synthesized and reported two sandwich-type polyanions: $(H_2tpy)(Hbpe)_3H[(VO)_6(SbW_9O_{33})_2]\cdot 2H_2O$ (tpy = 4-(2,3,4-tri(pyridin-4-yl)butyl)pyridine, bpe = 1,2-(4-pyridyl)ethane) and $(H_2tcy)_6(Hbpp)_6H_4[VW_{12}O_{40}][(VO)_6(SbW_9O_{33})_2]_3\cdot 30H_2O$ (tcy = 1,2,4,5-tetra(pyridin-4-yl)cyclohexanol).[12] Unusual in situ organic reactions involving C–C coupling were observed, regardless of the rigid bpe or flexible bpp. Interestingly, the organic cationic moieties in two compounds consist of two kinds of protonated molecules, and the tpy and tcy can be seen as dimers formed though in situ dehydrogenative coupling of bpe and bpp, respectively. The sandwich-type $[(VO)_6(SbW_9O_{33})_2]^{6-}$ polyanion played important roles in the formations of tpy and tcy.

As a continuous work, here we reported two new compounds $(H_2chtpy)_2[SiW_{12}O_{40}]$ (**1**) (chtpy= 1,3,4,6-tetra(4-pyridyl)cyclohexane-1,3-diol) and $[Co(Hbztpy)_2]H[AlW_{12}O_{40}]\cdot 3H_2O$ (**2**) (bztpy= 1,2,4,5-tetra(4-pyridyl)benzene), which had been hydrothermally synthesized and characterized. During the formation process of **1** and **2**, in situ organic reactions involving C－C coupling through dehydrogenative cyclodimerization from two flexible bpp molecules are occured. The tetradentate chtpy and bztpy serve as 4-connected nodes to form novel hydrogen bonding grids to accommodate the Keggin-type polyanions.

College of Chemistry and Material Science, Hebei Normal University, Shijiazhuang, 050024, China. E-mail: hanzg116@126.com

† Electronic Supplementary Information (ESI) available: Crystal CIF files, IR, XRD, ^1H NMR spectra and the other Figures.. See DOI: 10.1039/x0xx00000x

2. Experimental section

2.1 Materials and measurements

$Na_9H[\beta\text{-}SiW_9O_{34}]\cdot 23H_2O$ was prepared by published methods,[13] and other common reagents for synthesis were purchased and used as received. Elemental analyses (C, H, and N) were performed on a Perkin-Elmer 2400 CHN elemental analyzer. The metal contents were determined by inductively coupled plasma (ICP) analysis on a Perkin-Elmer Optima 3300DV ICP spectrometer. IR spectra were recorded in a KBr pellet with an FTIR-8900 IR spectrometer in the range of 400-4000 cm^{-1} region. Powder X-ray diffractions (XRD) were determined by a Bruker AXS D8 Advance diffractometer.

2.2 Preparation of 1-2

Synthesis of $(H_2chtpy)_2[SiW_{12}O_{40}]$ (1). A mixture of $Na_9H[\beta\text{-}SiW_9O_{34}]\cdot 23H_2O$ (200 mg, 0.08 mmol), $AgNO_3$ (150 mg, 0.88 mmol) or $CdCl_2\cdot 2H_2O$ (250 mg, 1.36 mmol), and bpp (25 mg, 0.13 mmol,) was dissolved in 10 mL 0.20M pH 3.5 buffer solution of NaAc/HAc at room temperature. Then, the suspension was put into a Teflon-lined autoclave and kept under autogenous pressure at 160 °C for 5 days. After slow cooling at 8 $°C\cdot h^{-1}$ to room temperature, orange-yellow block crystals were filtered and washed with distilled water (34% yield based on W). Elemental anal. Calcd (%) for $C_{52}H_{52}N_8O_{44}SiW_{12}$ (Mr = 3727.31): C, 16.75; H, 1.40; N, 3.01; W, 59.19. Found (%): C, 16.72; H, 1.38; N, 3.00; W, 59.22. Selected IR (KBr pellet, cm^{-1}): 3542m, 3100m, 1636s, 1506m, 1415m, 1015w, 972s, 922s, 883w, 795s, 534m.

Synthesis of $[Co(Hbztpy)_2]H[AlW_{12}O_{40}]\cdot 3H_2O$ (2). A mixture of $Na_2WO_4\cdot 2H_2O$ (250 mg, 0.75 mmol), $Al(NO_3)_3$ (96 mg, 0.45 mmol), $CoCl_2\cdot 6H_2O$ (93 mg, 0.39 mmol), and bpp (25 mg, 0.13 mmol,) was dissolved in 10 mL of distilled water at room temperature. When the pH value of the mixture was adjusted from 6.4 to 5.5 with 2 $mol\cdot L^{-1}$ HNO_3 solution, the suspension was put into a Teflon-lined autoclave and kept under autogenous pressure at 160 °C for 4 days. After slow cooling at 8 $°C\cdot h^{-1}$ to room temperature, orange-red block crystals were filtered and washed with distilled water (19% yield based on W). Elemental anal. Calcd (%) for $C_{52}H_{36}AlCoN_8O_{43}W_{12}$ (Mr = 3753.00): C, 16.52; H, 0.96; N, 2.88; Al, 0.72; Co, 1.57; W, 59.03. Found (%): C, 16.60; H, 0.95; N, 2.98; Al, 0.71; Co, 1.58; W, 58.85. Selected IR (KBr pellet, cm^{-1}): 3436s, 1636m, 1506w, 1046w, 957s, 889s, 804s, 766s.

2.3 X-ray crystallography

Crystal data of compounds were collected with the approximate dimensions 0.17 × 0.13 × 0.11 for **1** and 0.15 × 0.19 × 0.13 mm^3 for **2** on an SMART APEX II CCD Area Detector diffractometer at 296(2) K using graphite-monochromated Mo Kα radiation (λ = 0.71073 Å). The structures were solved by the direct methods and refined by the full-matrix least-squares method on F^2 with the SHELXTL crystallographic software package.[14] All the non-hydrogen atoms were refined anisotropically except for two water oxygen atoms (O1w, O2w) in **2**. The hydrogen atoms attached to carbon atoms were generated theoretically and refined isotropically with fixed thermal factors. The hydrogen atoms of hydroxyl groups were located from a difference Fourier map and refined with a fixed model in **1**. The protonated H atoms attached to nitrogen atoms in **1-2** had been fixed as riding modes. Positions of hydrogen atoms attached to water molecules were not located. The crystal data and structure refinement parameters for compounds **1-2** are summarized in Table 1. Some representative hydrogen bonding interactions are shown in Table 2. CCDC-1405995 (for **1**) and 1405996 (for **2**) contain the supplementary crystallographic data for this paper. These data can be obtained free of charge from The Cambridge Crystallographic Data Centre via www.ccdc.cam.ac.uk/data_request/cif (or from the Cambridge Crystallographic Data Centre, 12, Union Road, Cambridge C 1EZ, UK; fax: +44-1223/336-033; e-mail: deposit@ccdc.cam.ac.uk).

Table 1. Crystal data and structure refinement parameters for **1-2**.

Compounds	**1**（CCDC 1405995）	**2**（CCDC 1405996）
Formula	$C_{52}H_{52}N_8O_{44}SiW_{12}$	$C_{52}H_{44}AlCoN_8O_{43}W_{12}$
Mr	3727.19	3761.04
Crystal system	Monoclinic	Monoclinic
Space group	$P2_1/n$	$C2/c$
a [Å]	14.5284(19)	21.610(3)
b [Å]	15.755(2)	21.283(3)
c [Å]	16.910(2)	16.8259(19)
α [°]	90	90
β [°]	93.141(2)	99.207(2)
γ [°]	90	90
V [Å^3]	3865.0(8)	7638.9(16)
Z	2	4
Crystal size	0.19 × 0.17 × 0.13	0.17 × 0.15 × 0.13
GOF on F^2	1.040	1.069
Final *R* indices, R_1	0.0544	0.0730
$wR_2[I>2\sigma(I)]$	0.1148	0.1670
R indices, R_1	0.0802	0.0913
wR_2 (all data)	0.1299	0.1759

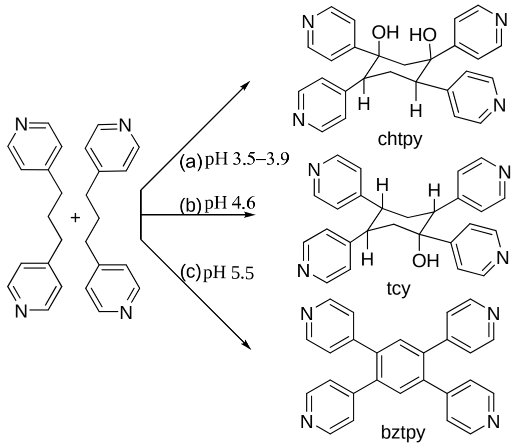

Scheme 1. In situ generation of chtpy, tcy and bztpy from bpp molecules.

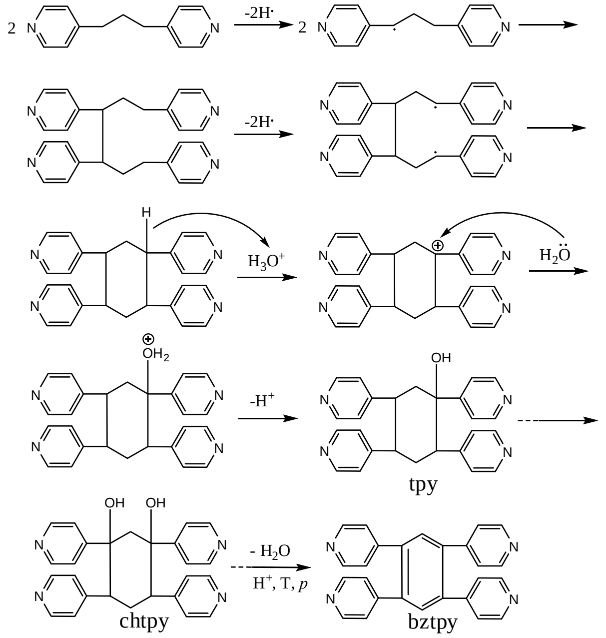

Scheme 2. The possible mechanism about in situ dimerization and dehydrogenative cyclodimerization of bpp molecules

3. Results and discussion

3.1 Synthesis

In this work, crystal **1** was synthesized by reacting $Na_9H[\beta\text{-}SiW_9O_{34}]$, $CdCl_2$ or $AgNO_3$, bpp with a given molar ratio in a buffer solution of NaAc/HAc at 160 °C for 5 days. A series of parallel experiments show that the formation of compound **1** is influenced by the reaction time, pH value, reaction temperature and metal salt species. If $CdCl_2$ or $AgNO_3$ was replaced with other metal salts, such as $Cu(NO_3)_2$, $Co(NO_3)_2$ or without any metal salt, no crystal was found. If $Na_9H[\beta\text{-}SiW_9O_{34}]\cdot 23H_2O$ was replaced by the simple metal salts Na_2WO_4 and Na_2SiO_3, the crystals were not also obtained. These results indicated that the raw materials are the key factor for the synthesis. Crystal **2** is a 3D covalent network consisting of Al-centered Keggin clusters and Co-ligand cations. One striking feature of this work is that bpp molecules dimerize into chtpy and bztpy in the two reaction cases (Scheme 1a, c), respectively. Carbon–carbon bond formation is crucially important for organic chemistry and is also the essence of organic synthesis. At present, it is very interesting to in situ generate chtpy and bztpy molecules from the dimerization of bpp molecules. In chtpy, the dehydrogenative coupling and hydroxylation of bpp into a hydroxylcyclohexane was observed. This kind of C–C bond formation was also reported in two MOFs.[15,16] The cyclohexane unit in chtpy is in a chair conformation. The lignd bztpy has a five-ring conjugated aromatic system: four pyridyl groups surround a central benzene nucleus. In most cases, the explanation of in situ reactions was ascribed to the coordination and catalysis of transition-metal ions. However no exact mechanisms of these molecular transformations are yet confirmed owing to the sealed conditions of the solvothermal reaction. An analysis on the conditions of synthesis reactions, one can find that the dehydrate resultants are benefited from the high pH values. To isolate the organic moiety from crystals, the crystals were placed in a mixture of alkaline solution (to destroy the strong hydrogen bonding network between anions and cations) and CH_2Cl_2 (to extract the organic moiety), and stirred for 2 days. Then the organic phase was separated from the reaction mixture and was concentrated to dryness. The ^1H NMR ([D$_6$]DMSO) result of powders showed that the bztpy could be always obtained whether the starting crystals were **1** or **2** (see Fig. S1). A transformation of chtpy to bztpy was completed under the alkaline condition. The possible mechanisms about in situ reactions as seen in Scheme 2, involving a series of free radical reactions in the dimerization route.

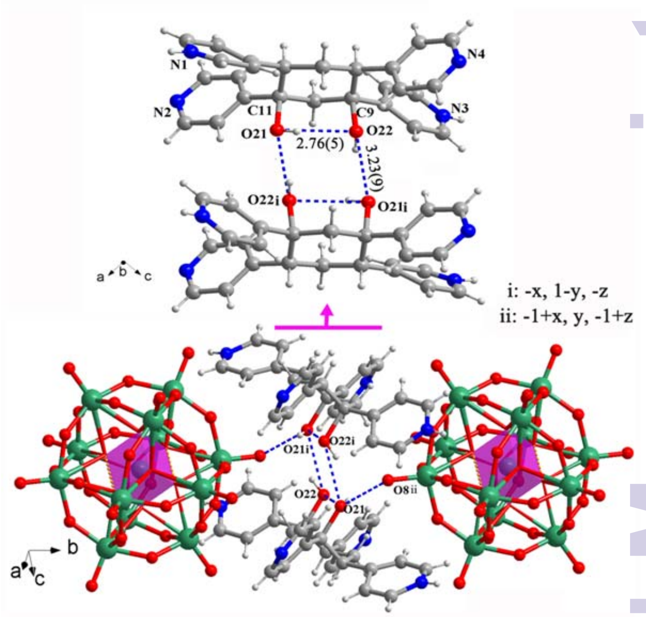

Fig. 1. Ball-stick view representations the dimer of chtpys and the intramolecular and intermolecular O-H…O hydrogen bonding interactions among the saturated Keggin-type $[SiW_{12}O_{40}]^{4-}$ and the cationic chtpy in **1**. Symmetry code: (i) -x, 1-y, -z; (ii) 1+x, y, -1+z.

3.2 Structure Description of 1

Single-crystal X-ray diffraction analysis revealed that the basic unit of compound **1** is constructed from one classical Keggin-type $[SiW_{12}O_{40}]^{4-}$ anion and two protonated chtpy cations (as shown in Fig. 1). The central Si atom lies on an inversion centre (1, 0, 1). The Si-O and W-O bond lengths are in their usual range. The five-ring organic chtpy can be seen as a dimer of two bpp molecules. The central six-membered ring of chtpy is formed through two new C-C bond couplings from four carbon atoms of $–(CH_2)_3–$ groups between two bpp molecules. The six C-C bond lengths of this ring fall in the range of 1.43(3)-1.53(2) Å, which are the characteristic distances of C-C single bond. Moreover, the cyclohexyl ring of the chtpy in **1** exhibit a slightly distorted chair conformation, and is bounded by two hydroxyl groups coming from the hydroxylation. The hydroxylations occur on the same side atoms C(11) and C(9) of the ring. The corresponding C-O bond lengths are 1.32(7) and

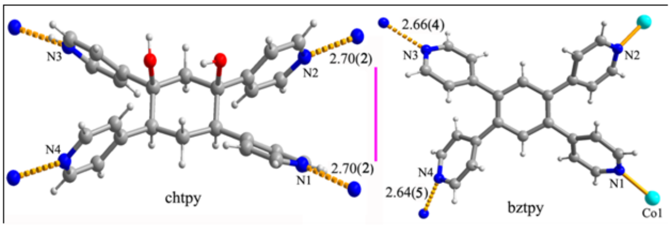

Fig. 2. A view showing the 4-connected mode of chtpy in **1** and bztpy in **2**.

1.62(3) Å. The four pyridyl groups along four different extension directions bond with the cyclohexyl ring. The hydroxyl oxygen atoms have the intramolecular (O(21)-H...O(22) = 2.76(5) Å) hydrogen bonding interactions to form a dimer of chtpys and intermolecular (O(22)-H...O(21i) = 3.23(9) Å), which further link $[SiW_{12}O_{40}]^{4-}$ clusters formed a 1D chain-like arranging by O-H...O hydrogen bonding interactions [O(8)...O(21i) = 2.79(3) Å. i: x, 3/2-y, -1/2+z], respectively.

The chtpy is protonated and exist as counterion to linkage anions into the supramolecular framework by the intermolecular N-H...O, O-H...O and C-H...O interactions. There are complex and effective hydrogen bonding interaction networks among protonated chtpy cations (N(2)...N(3i) = 2.70(2) Å], N(1)...N(4i) = 2.70(2) Å, see Fig. 2). Then, a structural feature is that cationic moiety form a lattice-type 4-connected layer through supramolecular N-H...N synthon (see Fig. 3a).[18] As mentioned above, two chtpys exist in the form of dimer. Therefore, it can be also seen as that the cationic moiety present a hydrogen bonding double-layered 4-connected sheet through N-H...N and O-H...O synthons (see Fig. 3b). The polyanions are orderly located at the lattice and fixed by O-H...O and C-H...O interactions [O(8)...O(21)] (see Fig. 3c). Some representative hydrogen bonding interactions are shown in Table 2. The adjacent double-layered 4-connected sheets are arranged in a dislocation mode each other. This kind of stacking pattern leads to that one anion is surrounded by six

Table 2. Representative intermolecular hydrogen bonding in crystals **1** and **2**.

D-H...A	D-H[Å]	H...A[Å]	D...A[Å]	D-H…A[°]
Compound **1**				
N(1)-H(1)...N(4^{i})	0.86	1.84	2.70(2)	176
N(3)-H(3)...N(2^{ii})	0.86	1.84	2.70(2)	174
O(21)-H(21A)...O(22)	0.82	2.19	2.76(5)	127
O(21)-H(21A)...O(8^{iii})	0.82	2.09	2.79(3)	143
C(10)-H(10A)...O(8^{iv})	0.97	2.47	3.41(2)	163
C(5)-H(5)…O(5^{v})	0.93	2.58	3.35(4)	140
C(16)-H(16)...O(5^{vi})	0.93	2.31	3.23(3)	173
O(22)-H(22A)···O(21^{vii})	0.82	2.45	3.23(9)	160
Symmetry codes: *i*= -1/2+x,1/2-y,1/2+z; *ii*= 1/2+x, 3/2-y,-1/2+z; *iii*= -1+x, y, -1+z; *iv*= 1-x, 1-y, 1-z; *v* = -1+x,y,-1+z; *vi*= 1/2-x, 1/2+y, 3/2-z; *vii* = -x, 1-y, -z.				
Compound **2**				
N(3)-H(3A)…N(3^{i})	0.86	1.82	2.66(4)	164
N(4)-H(4A)…N(4^{ii})	0.86	1.89	2.64(5)	146
C(7)-H(7)...O(1^{iii})	0.93	2.47	3.25(4)	141
C(12)-H(12)...O(21)	0.93	2.54	3.29(3)	137
C(23)-H(23)...O(10^{iv})	0.93	2.52	3.20(3)	130
Symmetry codes: *i* = 2-x,y,3/2-z; *ii* = 2-x,y,5/2-z; *iii* = x,1-y,1/2+z; *iv* = 1/2+x,-1/2+y,z.				

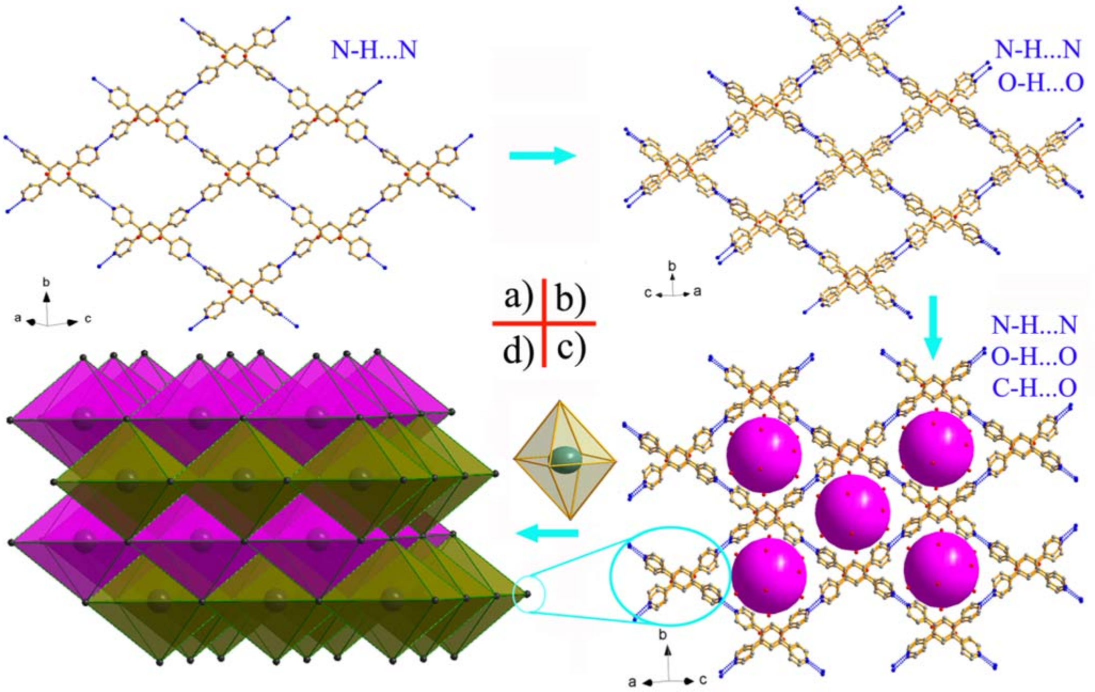

Fig. 3. a) The lattice-type 4-connected layer through supramolecular N-H...N synthon in **1**; b) the bilayer-like sheet through O-H...O interaction; c) a view shows that the Keggin anions are orderly filled in the centers of the 2D organic network and fixed by hydrogen bonding interactions of O-H...O and C-H...O; d) The stacking of organic octahedra building from Kegging type $[SiW_{12}O_{40}]^{4-}$ clusters and dimers of chtpy.

dimers of chtpy, which form an organic cage embedded with a Keggin-type cluster. If taking one dimer as the node, an interesting polyanion-centered organic octahedron is presented: four dimers residing on the same sheet construct the equatorial plane, and the other two dimers coming from up and down adjacent sheets are the vertexes. As shown in Fig. 3d, these octahedra link each other in corner-, edge-, and even face-shared modes. Evidently, the oxidative coupling of two bpp units is essential in establishing the 3D framework in compound **1**.

3.3 Structure Description of 2

The structural feature of **2** consists of a three-dimensional covalent net-like arrangement built upon Keggin-type $[AlW_{12}O_{40}]^{5-}$ anions and Co-ligand units (Fig. 4). The polyanion is a typical Keggin structure having a group element Al^{III} as central atom. It has a higher surface negative charge than those widely studied Keggin clusters with groups 14 (Si^{IV} and Ge^{IV}) and 15(P^{V} and As^{V}) elements as central atoms. The Al atom lies on an inversion centre (3/4, 3/4, 1). The central $\{AlO_4\}$ tetrahedron with Al-O bond lengths 1.69(3)-1.83(3) Å is crystallographically disordered with two orientations of a 1:1 ratio. Three groups of W-O bond lengths are in their usual range. The Co(1) atom lies on a twofold axis. The Co(II) center with a [4+2] mode is six-coordinated by four N donors from four bztpy ligands [Co(1)-N(1) = 2.19(2) Å, Co(1)-N(2) = 2.15(2) Å], and two O donors from two $[AlW_{12}O_{40}]^{5-}$ anions [Co(1)-O(12) = 2.13(2) Å], respectively. Therefore, the anion presents a bi-supported Keggin structure with two Co-O bonds.

Interestingly, the formation of **2** also involves an interesting organic transformation reaction. The tetradentate ligand bztpy in **2** is formed in situ hydrothermally via dehydrogenative cyclization coupling of two bpp molecules. Differently, the six carbon atoms in the central ring of bztpy are coplanar and the whole molecule presents a conjugated system. The corresponding C=C bond lengths are in the range of 1.36(4)-1.40(3) Å. Then, the ligand bztpy consists of five aromatic rings: one phenyl- and four pyridyl-groups. The five aromatic rings are not in a plane owing to the intramolecular tension. The bztpy can be seen as the product further dehydrating two water molecules from chtpy. Four pyridyl groups of bztpy form four bonding interaction with the adjacent ions or molecules: two of them are protonated and have supramolecular N-H…N hydrogen bonding interaction with two nearby bztpy ligands; the remaining two pyridyl groups are covalently bound to two Co(II) centers into the 1D chain-like $\{Co(bztpy)\}_\infty$ structure (see Fig. 4b).

For the sake of illustration, Fig. 5 clearly shows the 3D structural feature of **2** after simplifying the ligands and anionic clusters in the network linkage. Along the crystallographic *b* axis direction the polyanion and Co-ligand layers stack alternatively. Worthy of mention is that the cationic sheet consists of a double-layer Co-ligand structure and can be further divided to two single layers. As shown in Fig. 5b, the red and yellow are two colors used to highlight them. In fact, it is a 2D waved-like supramolecular layer (see Fig. 5c), in which the chains of $\{Co(bztpy)\}_\infty$ are linked through the N-H…N hydrogen bonding interactions [N(3)...N(3)' = 2.66(4) Å and N(4)...N(4)'' = 2.64(5) Å] among ligands. Each bztpy as a 4-connecting node involves in the construction of 2D layer via two covalent Co-N bonds and non-covalent N-H…N hydrogen bonds. These 2D layers are linked by Co-O bonds among inorganic and organic sheets into the 3D crystal framework of **2**. The Co(II) centers play a critical role in the covalent framework. A topological analysis on crystal structure indicates that the complete Schläfli notation for cobalt atoms in the infinite 3D net is short (6^6) and long (6^2, 6^2, 6^2, 6^2, 6^2, 6^2) (see Fig. 5d), respectively.

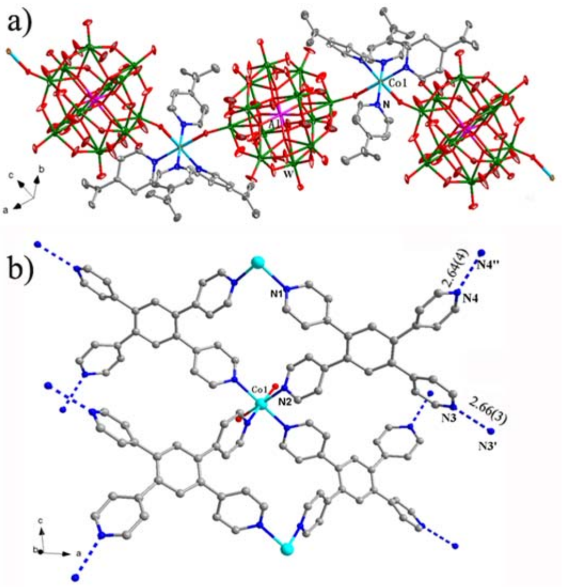

Fig. 4 a) A ORTEP view shows the linkage of anion and cation in **2**. The ligand was drawn partly for clarity. Ellipsoids are drawn at the 30% probability level; b) The immediate coordination environment around the Co(1) center and short distances of 2.66(3) Å for N3...N3'(2-x, y, 3/2-z) and 2.64(4) Å for N4...N4'' (2-x, y, 5/2-z) in **2**. All hydrogen atoms and guest water molecules are omitted for clarity.

3.4 IR spectra and XRD patterns

The IR spectra of compounds **1** and **2** are presented in Fig. S2. Characteristic bands at 972, 922, 880 and 795 cm^{-1} in **1**, 957, 889 and 804 cm^{-1} in **2** are attributed to ν($W=O_t$), and ν($W-O_b-W$) vibrations, respectively. Bands in the regions of 1100-1640 cm^{-1} are attributed to the organic chtpy and bztpy. The peak at 1636 cm^{-1} is attributed to the ν(C=N) and/or ν(C=C) vibration of pyridine and/or benzene ring groups. Furthermore, in IR spectrum of **1**, the peak at 1415 cm^{-1} indicates the characteristic peak of ν(C-O) in chtpy.

The simulative and experimental powder X-ray diffraction patterns of **1** and **2** are coincident, which confirm that the as-prepared compounds are pure (as shown in Fig. S3 in the Supporting Information). The difference in intensity between the experimental and simulated XRD patterns is due to the variation in the preferred orientation of the powder sample during collection of the experimental XRD data.

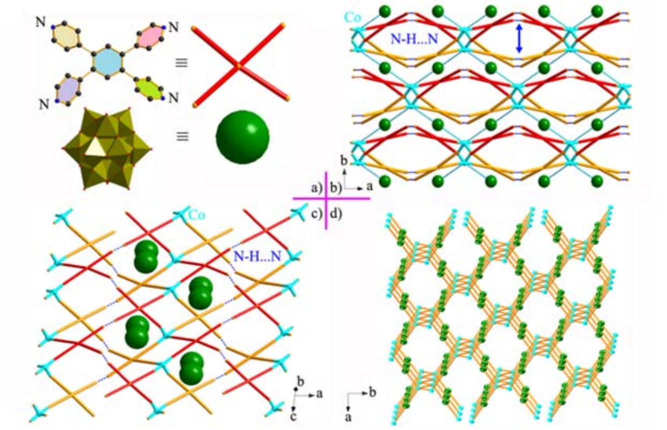

Fig. 5. a) The simplifications of bztpy and $[AlW_{12}O_{40}]^{5-}$ anions; b) a view showing the inorganic and organic sheets. The red and yellow are two colors used to highlight the double-layer Co-ligand structure; c) the 2D waved-like supramolecular layer of Co-ligand; d) The topological analysis on cobalt atoms in the infinite 3D net is short (6^6) and long (6^2, 6^2, 6^2, 6^2, 6^2, 6^2), respectively.

4. Conclusions

Two inorganic-organic supramolecular assemblies had been hydrothermally synthesized and characterized. Both two hybrids are built upon complex supramolecular contacts between inorganic polyanion and organic cation moieties. In the formation process of **1** and **2**, in situ organic reactions involving C-C coupling through dehydrogenative cyclodimerization from two flexible bpp molecules are observed. The tetradentate chtpy and bztpy serve as 4-connected nodes, leading to the novel structural topologies. The strong centered N-H…N (N…N = 2.6-2.7 Å) hydrogen bonding interactions link organic cations to form grid-type networks for capturing the pseudo-spherical Keggin-type anions. This work demonstrates that the in situ organic reaction with the presence of polyanion is a powerful method not only to generate new organic molecules, but also to represent a potential direction for construction of new hybrid frameworks through crystal engineering. Much work still needs to be done to account for the in situ reaction mechanism of organic molecules.

Acknowledgements

This work was financially supported by the Natural Science Foundation of China (No. 21341003), the Hebei Natural Science Foundation of China (No. B2015205116) and the Key Research Fund of Hebei Normal University (No. L2011Z06).

Notes and references

1 (a) X. M. Chen and M. L. Tong, *Acc. Chem. Res.*, 2006, **40(2)**, 162; (b) X. M. Zhang, *Coord. Chem. Rev.*, 2005, **249**, 1201.
2 (a) O. R. Evans and W. B. Lin, *Chem. Mater.*, 2001, **13**, 3009; (b) S. M. Humphrey, R. A. Mole, J. M. Rawson and P. T. Wood, *Dalton Trans.*, 2004, 1670.
3 J. Burgess and C. D. Hubbard, *Adv. Inorg. Chem.*, 2003, **54**, 71
4 (a) Z. G. Han, Y. L. Zhao, J. Peng and C. J. Gomez-Garcia, *Inorg. Chem.*, 2007, **46(14)**, 5453; (b) Z. G. Han, Y. Z. Gao, X. L. Zhai and H. H. Song, *Inorg. Chem. Commun.*, 2007, **10**, 1079.
5 (a) J. Y. Lu, *Coord. Chem. Rev.*, 2003, **246**, 327; (c) L. Han, X. Bu, Q. Zhang and P. Feng, *Inorg. Chem.*, 2006, **45**, 5736; (c) J. Zhang, T. Wu, P. Y. Feng and X. H. Bu, *Chem. Mater.*, 2008, **20**, 5457.
6 A. Dolbecq, E. Dumas, C. R. Mayer and P. Mialane, *Chem. Rev.*, 2010, **110**, 6009.
7 (a) D. L. Long, E. Burkholder and L. Cronin, *Chem. Soc. Rev.*, 2007, **36**, 105; (b) C. Streb, D. L. Long and L. Cronin, *CrystEngComm*, 2006, **8**, 629; (c) D. W. Yan, J. Fu, L. Zheng, Z. B. Zhang, Y. Xu, X. L. Zhu and D. R. Zhu, *CrystEngComm*, 2011, **13**, 5133.
8 (a) H. J. Lv, Y. V. Geletii, C. C. Zhao, J. W. Vickers, G. B. Zhu, Z. Luo, J. Song, T. Q. Lian, D. G. Musaev and C. L. Hill, *Chem. Soc. Rev.*, 2012, **41**, 7572; (b) X. L. He, Y. P. Liu, K. N. Gong, Z. Han and X. L. Zhai, *Inorg. Chem.*, 2015, **54**, 1215; (c) K. N. Gong, W. J. Wang, J. S. Yan and Z. G. Han, *J. Mater. Chem.*, A, 2015, **3**, 6019.
9 M. P. Suh, H. J. Park, T. K. Prasad and D. W. Lim, *Chem. Rev.*, 2012, **112**, 782.
10 (a) C. Dey and R. Banerjee, *ChemPhysChem*, 2013, **14**, 1009; (b) S. Hu, Z. S. Meng and M. L. Tong, *Cryst. Growth Des.*, 201 **10**, 1742; (c) W. Wei, K. Yu, Z. H. Su, Y. Yu, B. B. Zhou and C. C Zhu, *Inorg. Chem. Commun.*, 2012, **17**, 21.
11 (a) J. S. Yan, K. N. Gong, X. L. Xue, X. L. He, C. Zhao, Z. G. Han and H. T. Yu, *Eur. J. Inorg. Chem.*, 2014, 5969; (b) L. Han, W. N. Zhao, Y. Zhou, X. Li, and J. G. Pan, *Cryst. Growth Des.*, 2008, 3504; (c) N. F. Zheng, X. H. Bu and P. Y. Feng, *J. Am. Chem. Soc.*, 2002, **124**, 9688.
12 Z. G. Han, Q. X. Zhang, Y. Z. Gao, J. J. Wu and X. L. Zhai, *Dalton Trans.*, 2012, **41**, 1332.
13 A. Téazéa, G. Hervé, R. G. Finke and D. K. Lyon, *Inorg. Synth.*, 1990, **27**, 85-96.
14 (a) G. M. Sheldrick, *SHELXS-97, Program for Crystal Structure Solution*; (b) *SHELXL-97, Program for Crystal Structure Refinement*, University of Göttingen, Göttingen, Germany, 1997.
15 J. X. Meng, X. L. Wang, E. B. Wang, Y. G. Li, C. Qin and X. X. Xu *Inorg. Chim. Acta*, 2008, **361**, 2447.
16 L. X. Sun, Y. Qi, Y. X. Che, S. R. Batten and J. M. Zheng, *Cryst. Growth Des.*, 2009, 2995.
17 F. H. Allen, O. Kennard, D. G. Watson, L. Brammer, A. G. Orpen and R. Taylor, *J. Chem. Soc., Perkin Trans.*, 1987, **2**, S1-S19.
18 Q. J. Kong, C. X. Zhang and Y. G. Chen, *J. Struct. Chem.*, 2012, **53**, 967.

Table of contents entry:

Grid-type hydrogen bonding network of organic cations are to capture the pseudo-spherical Keggin-type anionic clusters.